ASTFE
American Society
of Thermal and Fluids Engineers

Proceedings of the 2nd Thermal and Fluid Engineering Conference, TFEC2017
4th International Workshop on Heat Transfer, IWHT2017
April 2-5, 2017, Las Vegas, NV, USA

TFEC-IWHT2017-17541

EXPERIMENTAL INVESTIGATION OF THE HEAT TRANSFER IN A HORIZONTAL MINI-TUBE WITH THREE DIFFERENT INLET CONFIGURATIONS

Hou-Kuan Tam[1*], Lap-Mou Tam[1,2], Afshin J. Ghajar[3], Qian Wang[1]

[1]Department of Electromechanical Engineering, Faculty of Science and Technology, University of Macau, Macau SAR, China.
[2]Institute for the Development and Quality, Macau SAR, China.
[3]School of Mechanical and Aerospace Engineering, Oklahoma State University, Stillwater, Oklahoma, USA.

ABSTRACT

In the traditional heat exchanger, the inlet configuration entering the straight tube include the sharp-edged contraction, re-entrant inlet, bell-shape nozzle, and different angle bends. For the macro-tube, the effect of different inlet configurations on heat transfer in the laminar, transition, and turbulent regime can be found in the open literature. However, those information has not been well studied in the smaller diameter tubes such as the mini-tube and micro-tube. Therefore, an experimental setup was built for this study to measure the mini-tube heat transfer under the uniform wall heat flux boundary condition.

In this study, heat transfer was measured in a test section fitted with a horizontal mini-tube of 2 mm inner diameter. Three inlet configurations (straight tube length, 90^o bend, and 180^o bend) were used in this study. The entire experiment covered the Reynolds number range between 900 and 3000. From the heat transfer results, the heat transfer characteristics from the laminar to upper transition regions was observed. Regardless of the inlet type, the influence of buoyancy on laminar heat transfer was present in the mini-tubes. However, the start of transition was inlet-dependent. From the entrance to fully developed region, the laminar heat transfer of the 90^o and 180^o bends was observed to be higher than that of straight tube length. Moreover, the 180^o bend had a slightly higher laminar heat transfer than the 90^o bend in the fully developed region.

KEY WORDS: Heat Transfer, Mini-tube, Inlet configurations

1. INTRODUCTION

Advances in micro-fabrication techniques have resulted in miniaturization of technology in almost all fields of engineering and bio-mechanics [1]. To design the devices such as miniature heat exchangers, pumps, or sensors, the understanding of the heat transfer inside the small scale tubes or channels is required. Due to the importance of investigating heat transfer inside the mini- and micro-tubes, Krishnamoorthy et al. [1] and Celeta [2] reviewed the published research works done on heat transfer in the micro-tubes and channels. According to their reviews, the single-phase heat transfer in the micro-tubes can be well predicted by the conventional correlations of macro-tubes. Celeta [2] stated that the incorrect heat transfer data analysis in the micro-tubes was due to the scale-effects, such as viscous dissipation, thermal entrance effect and axial length of the test section. Once these effects were taken into consideration, the heat transfer data for the micro-tubes should follow the conventional correlations. Krishnamoorthy et al. [1] pointed out that effects of surface roughness, diameter and heat flux magnitude could not be overlooked and thus the laminar heat transfer of the mini- and micro-tubes could not be concluded to be equal to the conventional value of Nu = 4.364. Based

*Corresponding Author: hktam@umac.mo

on the review works of [1, 2], the past studies seldom discussed the effect of inlet on heat transfer inside the mini- and micro-tubes. However, the effect of inlet on laminar and transition regions heat transfer was observed in the macro-tubes [3-6].

In the macro-tube studies [3-5], it was clearly shown that the start and end of transition and the heat transfer characteristics in the transition region were influenced by three different inlet configurations, re-entrant, square-edged, and bell-mouth, installed before the horizontal plain tube with an inner diameter of 15.8 mm. Moreover, for the bell-mouth inlet, an unusual behavior in the Nu vs. x/D_i curve was observed in the transition and turbulent regions. Such unusual behavior for bell-mouth inlet was also observed in the micro-fin tubes with an inner diameter of around 15 mm [6]. Recently, Dirker et al. [7] analyzed the inlet effect on heat transfer and friction factor inside the micro-and mini-channels of 0.57, 0.85, and 1.05 mm in hydraulic diameter. The inlets used were sudden contraction, bell-mouth, and swirl inlets. They concluded that the heat transfer and friction factor behaviors, especially, in the transition region, were influenced by the inlet configuration.

Besides of the above-mentioned inlets, bending inlets with different angles are also used in the traditional heat exchanger and the effect of the bends on heat transfer in macro-tubes can be found in some experimental studies [8-12]. Practically, the bending entrance before a straight tube is also important in miniature heat exchangers. However, those information has not been well studied in the smaller diameter tubes such as the mini-tube and micro-tube. Therefore, the main objective of this experimental study is to investigate the effect of the inlets with various angles of bends (90^o bend and 180^o bend) on heat transfer characteristics inside the mini-tube in the laminar and upper transition regions.

2. EXPERIMENTAL SETUP

The experimentation for this study was performed using a relatively simple but highly effective apparatus. The apparatus used was designed with the intention of conducting highly accurate heat transfer measurements. The apparatus consists of four major components. These are the fluid delivery system, the flow meter, the test section assembly, and the data acquisition system. An overall schematic for the experimental test apparatus is shown in Fig. 1.

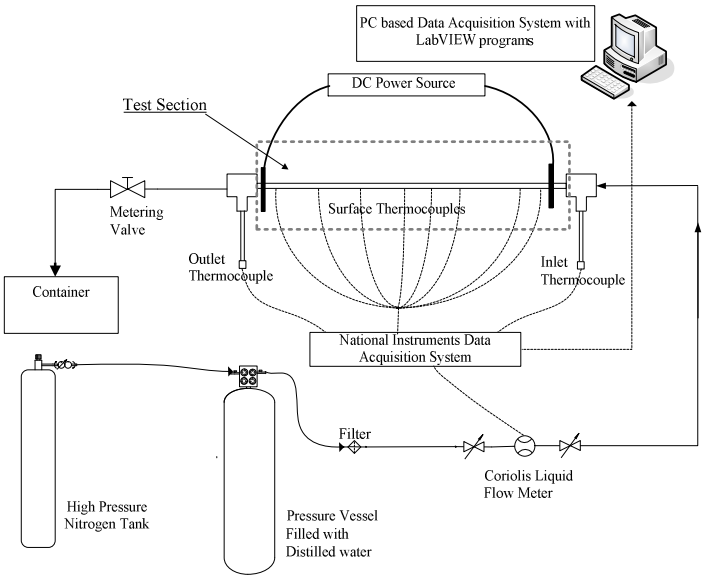

Fig. 1 Schematic diagram of heat transfer measurement system.

The working fluid used in this study is distilled water. As the pressurized nitrogen is fed into the pressure vessel, the distilled water is forced out of the pressure vessel, and through the flow meter array and test section. Flow rate of the water entering the array is further regulated using a metering valve and is measured by a Coriolis liquid flow meter. After the working fluid passes through the flow meter, fluid enters the test section assembly. In the test section assembly, the entire straight tube with different inlets are arranged between the fittings of inlet and outlet thermocouples.

Kandlikar and Grande [13] defined the channel with the hydraulic diameter of larger than 3 mm as the 'conventional channel' and the channel with the diameter range between 3 mm and 0.2 mm as the 'mini-channel'. In this study, the test section was a horizontal stainless circular mini-tube with 2 mm inside diameter and 3.2 mm outside diameter. The total length of the heating section (L_t) was 680 mm, providing a maximum heating length-to-inside diameter ratio (L_t/D_i) of 340. As shown in Fig. 2, the tolerance of the diameter of the tested tubes measured by Scanning Electron Microscope (SEM, S3400N, HITACHI) was ± 0.12 mm. The average roughness measured by Atomic Force Microscope (AFM, XE7, Park-Systems) was 0.63 μm.

As shown in Fig. 1, electric copper wires were soldered on to both ends of the test tube. A DC power supply was used to provide the uniform wall heat flux boundary condition. The voltage was measured at the soldered positions of the tube and the current was measured from the electric wire connected from the soldered position to the DC power supply. The range of wall heat flux of this study was from 11 kW/m^2 to 32 kW/m^2. For the temperature measurements, the inlet and exit bulk temperatures were measured by means of thermocouple probes (Omega TMQSS-125U-6) placed before and after the test section. Also, for the heat transfer experiments, the thermocouples (Omega 5TC-TT-T-40-36) were attached with the adhesive pads (Omega TAP) along the test section. All the thermocouples and thermocouple probes were calibrated by a NIST-calibrated thermocouple probe (±0.22°C) and an Omega HCTB-3030 constant temperature circulating bath. Therefore, the temperature sensors were as accurate as ±0.22°C.

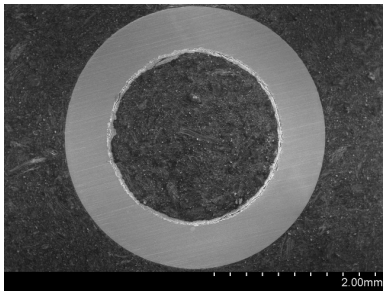

Fig. 2 SEM measurement of the stainless steel tube.

Figures 3 (a-d) show the three types of inlet configurations (straight tube, 90^o bend, and 180^o bend) installed before the horizontal tube and the arrangement of the thermocouples (TC) on the test section. In Fig. 3(a), there is a straight tube length arranged horizontally before the heating section. In Figs. 3 (b & c), the 90^o and 180^o bends are formed by bending straight tube and the bends and the heating section are placed horizontally on the test table. The curvature ratio (R/r_i) of the bends is 12.5. To ensure a hydrodynamically developed flow condition, a certain length of straight tube is arranged before each bend. Fig. 3(d) shows the arrangent of the two themocouples TC_{top} and TC_{bottom} (one on the top and one on the bottom of the tube) placed at each measuring station along the straight length of the mini-tube. After installation of the thermocouples, the tested tube was covered by self-adhesive elastomeric insulating material.

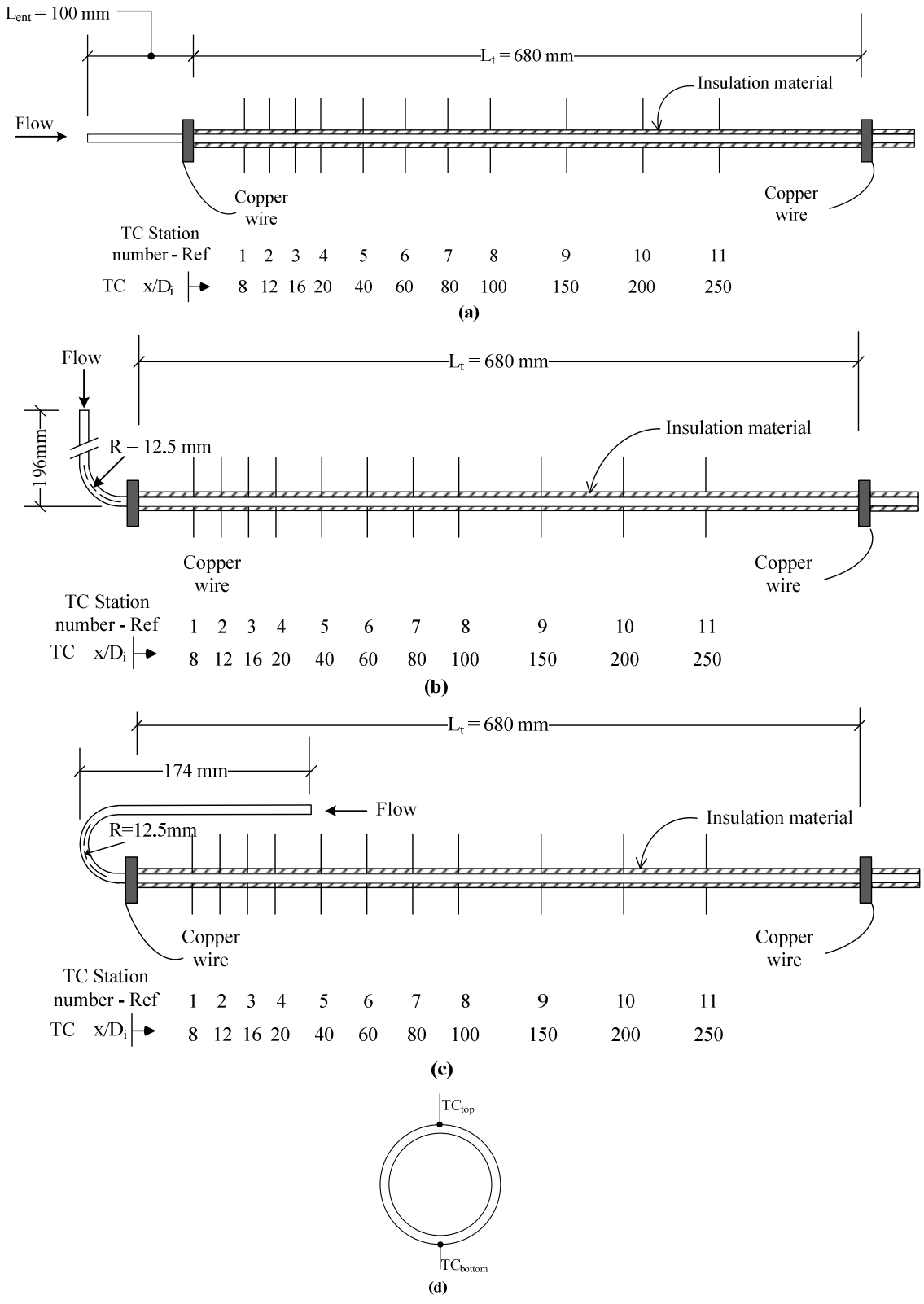

Fig. 3 Test sections with different horizontal inlets and thermocouples: (a) straight tube length; (b) 90^o bend, (c) 180^o bend, (d) top and bottom thermocouples at each station.

From the local peripheral wall temperature measurements at each axial location, the inside wall temperatures and the local heat transfer coefficients were calculated by the method shown in [14]. In these calculations, the axial conduction was assumed negligible (RePr > 5400), but peripheral and radial conduction of heat in the tube wall were included. In addition, the bulk fluid temperature was assumed to increase linearly from the inlet to the outlet. Also, the dimensionless numbers, such as Reynolds, Prandtl, Grashof, and Nusselt numbers, were computed by the computer program developed by [14]. The range of Reynolds number for this study was from 900 to 3000. Heat balance errors were calculated for all experimental runs by taking a percent difference between two methods of calculating the heat addition. The product of the voltage drop across the test section and the current carried by the tube was the primary method, while the fluid enthalpy rise from inlet to exit was the secondary method. In all cases the heat balance error was less than ±17%. The primary method was the one used in the computer program [14] for all heat flux and heat transfer coefficient calculations. Except the first location ($x/D_i = 8$), the maximum uncertainty of the heat transfer coefficients over the entire range of Reynolds numbers was less than 11%. At the first location ($x/D_i = 8$), the uncertainty of the heat transfer coefficients was up to 19%. It was because the surface temperature at that location was not high enough to obtain a better uncertainty due to a lower heat input to the tube. That can be improved by adding more heat into the tube. The calculation method was based on Kline and McClintock [15]. The Kline and McClintock method was used to determine the uncertainty of a calculation given certain measurements and the tolerances on those measurements. In this study, those measurements such as the measurements of bulk and surface temperatures, voltage, current, tube diameter and heated length were involved in the calculation of the uncertainty of the heat transfer coefficient.

For data acquisition, a National Instruments SCXI-1000 data collecting system was used. All digital signals from the flow meter and thermocouples were acquired and recorded by the Windows-based PC with a self-developed LabVIEW program.

3. RESULTS AND DISCUSSION

To verify the new experimental setup, experiments with the straight tube length were conducted first. Fig. 4 shows the comparison of the current 2 mm tube fully developed heat transfer data (at the $x/D_i = 200$) with the data of Ghajar and Tam [3] (at the $x/D_i = 200$) for a 15.8 mm stainless steel tube with square-edged and re-entrant inlets. Basically, the present laminar and lower transition heat transfer data could follow the data trend of [3]. Especially, the start of transition and transition trend of the current data were closer to the re-entrant inlet data although the different tube size and inlet were used in the current and past studies. Therefore, the experimental setup and the heat transfer data were confirmed to be reliable. In the figure, it should be noted that the parallel shift from the classical fully developed value of Nu = 4.364 for the uniform wall heat flux boundary condition in the laminar region is due to the buoyancy effect [3, 5].

After the verification of the experimental setup, heat transfer data were measured in the three test tubes with different inlet configurations. The heat transfer results of the three different inlets are shown in Fig. 5. In the figure, it can be seen that almost all of the heat transfer data of those tubes in the laminar region collapse into a single line parallel to the classical laminar fully developed line (Nu = 4.364 for uniform wall heat flux boundary condition). The shift from the classical value is caused by the buoyancy effect. According to Ghajar and Tam [3] and Tam and Ghajar [5], the buoyancy effect for the tested tube can also be examined by the ratio of the heat transfer coefficient of the top and bottom (h_t/h_b) measured by the top and bottom thermocouples at each station. The ratio of h_t/h_b should be close to unity (0.8–1.0) for forced convection and is much less than unity (<0.8) for a case in which mixed convection exists. In the current study, the ratio of h_t/h_b in the fully developed region such as x/D_i of 200 is much lower than 0.8 so the upward shift from the classical laminar line is confirmed to be caused by the buoyancy effect.

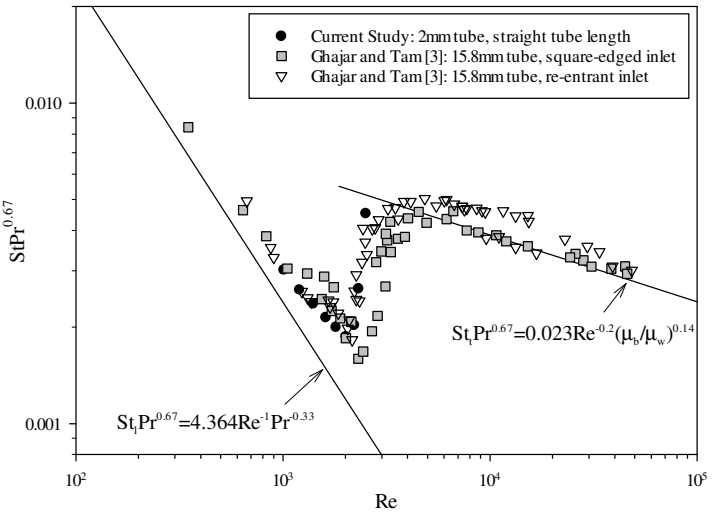

Fig. 4 Comparison of the present heat transfer data with the experimental data of [3].

As seen in Fig. 5, the start of transition for those inlets is defined as the point of sudden departure from the laminar Nu line parallel to the classical Nu = 4.364 line. The start of transition for heat transfer (with uniform wall heat flux boundary condition) in the tested tube for the three inlet configurations (straight tube length, 90^o bend, and 180^o bend inlets) were established and the transition Reynolds numbers for heat transfer are summarized in Table 1. Referring to Fig. 5 and Table 1, it can be observed that the start of transition is found to be inlet dependent. The start of transition Reynolds number for each inlet is determined to be about 2000 for the straight tube length, 2200 for the 90^o bend, and 2500 for the 180^o bend inlets. The results indicate that the larger bending angle inlet delays the start of transition when the straight tube length is treated as the base case. The delay of start of transition by the bend inlet may be explained as the less disturbance due to a momentum flow through the bend. After the start of transition, the transition trends for those inlets move upward in different ways.

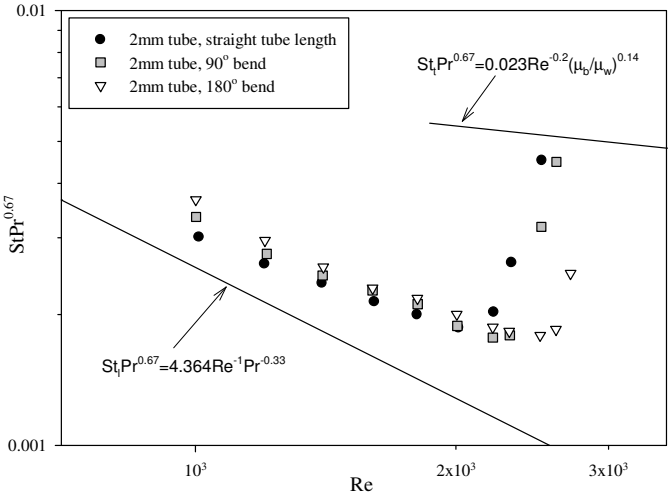

Fig. 5 Heat transfer characteristics for the three different inlets at x/D_i of 200.

Table 1 Start of transition for the three different inlets at x/D_i of 200.

Tube, Inlet	Heat Transfer	
	Re_{start}	$StPr^{0.7}$
Straight tube length	2014	$1.86e^{-3}$
90° bend	2206	$1.77e^{-3}$
180° bend	2502	$1.79e^{-3}$

Figure 6 shows the variation of local Nusselt number along the tube length (x/D_i) in the laminar and upper transition regions for the tubes with the three inlet configurations. As shown in the figure, for the laminar region, the local Nusselt number first decreases along the tube and then stays constant after x/D_i of 60 regardless of the type of inlet. The 90° bend and 180° bend inlets seem to have a higher Nusselt number in the entrance region (at the x/D_i of less than 60). This may be explained by the fact that the centrifugal force developed in the bend increased the velocity gradient at the bottom region of the circular pipe and thus produced the higher heat transfer rate. A further comparison for the three inlets in the laminar region is required. Referring to Fig. 6, while the Reynolds number exceeds the start of transition (approximately, 2000 for straight tube length, 2200 for 90° bend, and 2500 for 180° bend), the local transitional Nusselt number first decreases along the tube, reaches the minimum value at the x/D_i of around 60 and then increases.

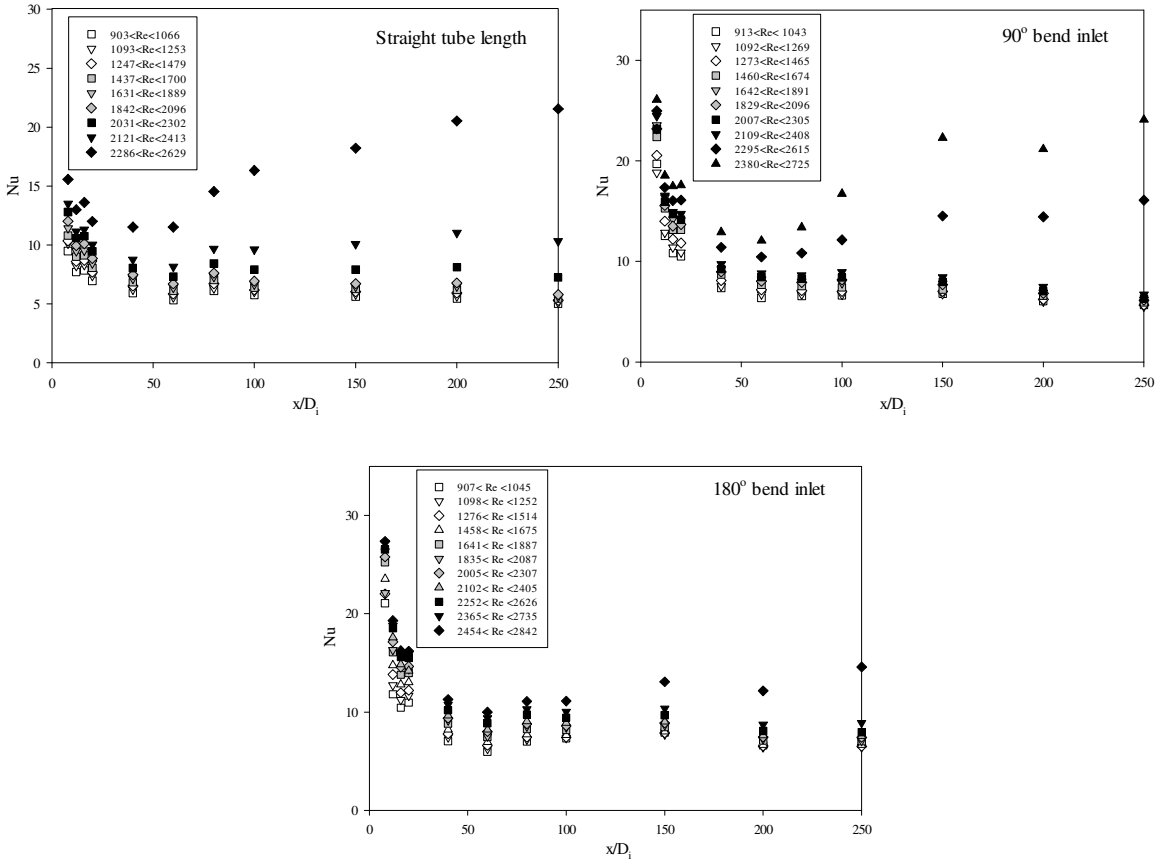

Fig. 6 Variation of local Nusselt number with length for the tested tubes with the different inlets.

Figure 7 shows the comparison of the variation of local Nusselt number along the tube length (x/D_i) in the laminar region for the three inlet configurations. As shown in Fig. 7, for all three inlets, the local Nusselt number first decreases along the tube and then stays fairly constant after x/D_i of 60. However, it is obvious that the local heat transfer coefficients for the entire tube length for both of the bend inlets is higher than that of the straight tube length inlet. Moreover, after the x/D_i of 60, the local heat transfer coefficients of the test tube with the 180^o bend inlet is slightly higher than that of the 90^o bend inlet. It is because a protruding curve trend is produced by the 180^o bend inlet at the x/D_i between 60 to 200. The special curve trend may be caused by the heat transfer enhancement by the complicated flow out from the 180^o bend inlet. It is also interesting to note the behavior of the 180^o bend inlet in the entrance region (for x/D_i of around 20), this could be possibly as a result of a stall region on the inside of the bend. The flow conditions affected by the presence of round bends at the entrance are complex. The velocity distribution is no longer symmetrical about the axis of the pipe. Certainly, a better understanding of the heat transfer enhancement is required with the flow phenomena of 'bend'.

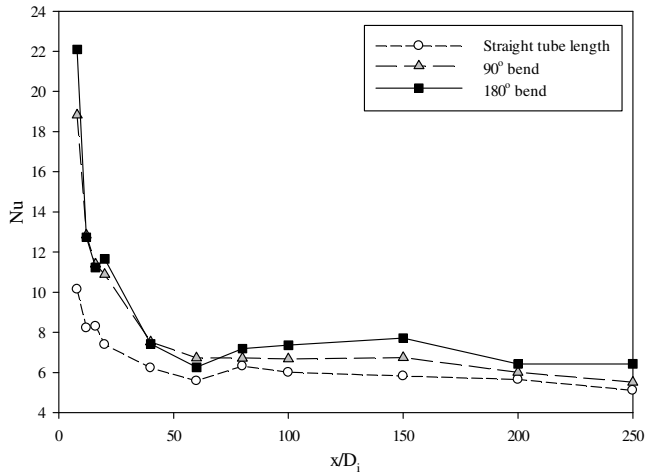

Fig. 7 Comparison of variation of local Nusselt number with length of the three different inlets in the range of the Reynolds number of 1092 and 1269.

4. CONCLUSIONS

In this study, heat transfer for the horizontal mini-tube with three different inlet configurations were obtained under uniform wall heat flux boundary condition. From the results, the following conclusions can be made:

- For the mini-tubes with three types of inlets, the buoyancy effect was present in the laminar region.
- For the mini-tubes, the start of transition was inlet dependent. The straight tube length inlet had the earliest start of transition and the 180^o bend inlet had the latest one. The 90^o bend inlet fell in between.
- Regardless of the type of inlet, the similar local Nusselt number behavior was observed in the laminar and upper transition regions and the entry length was almost at the x/D_i of 60.
- In the laminar region, the local heat transfer coefficients for the entire tube length for both of the bend inlets is higher than that of the straight tube length inlet. In the fully developed region, the higher heat transfer due to a larger bend angle was observed.

ACKNOWLEDGMENT

This research is supported by the Institute for the Development and Quality, Macau.

NOMENCLATURE

c_p	specific heat of the test fluid evaluated at T_b	(J/(kg·K))
D_i	inner diameter	(mm)
h	fully developed peripheral heat transfer coefficient	(W/(m^2·K))
h_b	local peripheral heat transfer coefficient at the bottom of tube	(W/(m^2·K))
h_t	local peripheral heat transfer coefficient at the top of tube	(W/(m^2·K))
k	thermal conductivity evaluated at T_b	(W/(m^2·K))
L_{ent}	entrance length before the heating length of the test section	(mm)
L_t	heating length of the test section	(mm)
Nu	local average or fully developed peripheral Nusselt number [= h·D_i /k]	
Pr	local bulk Prandtl number [= c_p·μ_b/k]	
R	radius of bend	(mm)
Re	local bulk Reynolds number [=ρ·V·D_i /μ_b]	
r_i	inner radius	(mm)
St	local average or fully developed peripheral Stanton number [= Nu/(Pr·Re)]	
T_b	local bulk temperature	(ºC)
T_w	local inside wall temperature	(ºC)
V	average velocity in the test section	(m/s)
x	local axial distance from the start point of heating	(m)

Greek Symbols

ε	Average surface roughness	(μm)
μ_b	absolute viscosity at T_b	(Pa×s)
μ_w	absolute viscosity at T_w	(Pa×s)
ρ	density of the test fluid evaluated at T_b	(kg/m^3)

Subscripts

l	laminar
t	turbulent

REFERENCES

[1] Krishnamoorthy, C., Rao, R. P., and Ghajar, A. J., "Single-Phase Heat Transfer in Micro-Tubes: A Critical Review", *Proceedings of the 2007 ASME-JSME Thermal Engineering Summer Heat Transfer Conference*, Vancouver, British Columbia, Canada, July 8-12, (2007).

[2] Celata G.P., Single and two phase flow heat transfer in micropipes, *5th European Thermal-Sciences Conference, The Netherlands*, (2008).

[3] Ghajar, A. J. and Tam, L. M., "Heat transfer measurements and correlations in the transition region for a circular tube with three different inlet configurations", *Experimental Thermal and Fluid Science*, 8(1), pp. 79-90, (1994).

[4] Tam, L. M., and Ghajar, A. J., "The unusual behavior of local heat transfer coefficient in a circular tube with a bell-mouth inlet," *Experimental Thermal and Fluid Science, 16*(3), 187-194, (1998).

[5] Tam, L. M., and Ghajar, A. J., "Transitional Heat Transfer in Plain Horizontal Tubes," *Heat Transfer Engineering, 27*(5), 23-38, (2006).

[6] Tam, H. K., Tam, L. M., Ghajar, A. J., Sun, C., and Lai, W. K., "Experimental Investigation of the Single-Phase Heat Transfer in a Horizontal Internally Micro-Fin Tube with Three Different Inlet Configurations," Proceedings of ASME 2012 Summer Heat Transfer Conference, July 2012, Puerto Rico, USA, (2012).

[7] Dirker J., Meyer, J. P., and Garach, D. V., "Inlet Flow Effects in Micro-channels in the Laminar and Transitional Regimes on Single-phase Heat Transfer Coefficients and Friction Factors," *International Journal of Heat and Mass Transfer*, 77, 612-626, (2014).

[8] Boelter, L. M. K., Young, G., and Iversen, H. W., *NACA (now NASA) TN 1451*, Washington, (1948).

[9] Kays, W. H., Crawford, M. E., and Weigand, B., *Convective Heat and Mass Transfer*, 4th Edition, McGraw-Hill, (2005).

[10] Abdelmessih, A. N. and Bell, K. J., "Effect of Mixed Convection and U-Bends on the Design of Double-Pipe Heat Exchangers," *Heat Transfer Engineering*, 20(3), (1999).

[11] Hrnjak, P. S. and Hong, S. H., "Effect of Return Bend and Entrance on Heat Transfer in Thermally Developing Laminar Flow in Round Pipes of Some Heat Transfer Fluids with High Prandtl Numbers," *Journal of Heat Transfer*, 132(6), (2010).

[12] Kakac, S., Shah, R. K., and Aung, W., *Handbook of Single-Phase Convective Heat Transfer*, Wiley, New York, 1987.

[13] Kandlikar, S. G. and Grande, W. J., "Evolution of microchannel flow passages - thermohydraulic performance and fabrication technology," *Proceedings of IMECE2002 ASME International Mechanical Engineering Congress & Exposition November 17-22, 2002,* New Orleans, Louisiana, (2002).

[14] Ghajar, A. J. and Kim, J., "Calculation of local inside-wall convective heat transfer parameters from measurements of the local outside-wall temperatures along an electrically heated circular tube," *Heat Transfer Calculations*, edited by Myer Kutz, McGraw-Hill, New York, NY, pp. 23.3-23.27, (2006).

[15] Kline, S. J., and McClintock, F. A., *Describing Uncertainties in Single Sample Experiments*, Mech. Eng., 75, pp. 3-8, (1953).